



Deep-Learning Framework to Detect Lung Abnormality – A study with Chest X-Ray and Lung CT Scan Images

Abhir Bhandary^a, G. Ananth Prabhu^b, V. Rajinikanth^{c,*}, K. Palani Thanaraj^c, Suresh Chandra Satapathy^d, David E. Robbins^e, Charles Shasky^f, Yu-Dong Zhang^g, João Manuel R. S. Tavares^h, N. Sri Madhava Raja^c

^aDepartment of Information Science Engineering, NMAM Institute of Technology, Nitte, Karnataka 574110, India

^bDepartment of Computer Science Engineering, Sahyadri College of Engineering & Management, Mangaluru 575007, India

^cDepartment of Electronics and Instrumentation Engineering, St. Joseph's College of Engineering, Chennai- 600 119 Tamilnadu, India

^dSchool of Computer Engineering, Kalinga Institute of Industrial Technology (Deemed to Be University), Bhubaneswar, 751024, Odisha, India

^eSchool of Public Health, Department of Health Informatics and Information Management, Samford University, Birmingham, AL, USA

^fVisiting Professor, Department of Health Administration, VCU/KMU EMHA Program, Medical College of Virginia, Virginia Commonwealth University, Richmond, VA, USA

^gDepartment of Informatics, University of Leicester, Leicester LE1 7RH, UK

^hInstituto de Ciência e Inovação em Engenharia Mecânica e Engenharia Industrial, Departamento de Engenharia Mecânica, Faculdade de Engenharia, Universidade do Porto, Porto, Portugal

ABSTRACT

Lung abnormalities are highly risky conditions in humans. The early diagnosis of lung abnormalities is essential to reduce the risk by enabling quick and efficient treatment. This research work aims to propose a Deep-Learning (DL) framework to examine lung pneumonia and the cancer. This work proposes two different DL practices to evaluate the considered problem: (i) The initial DL method, named a modified AlexNet (MAN), is implemented to classify chest X-Ray images into normal and pneumonia class. In the MAN, the classification is implemented using with Support Vector Machine (SVM), and its performance is compared against Softmax. Further, its performance is validated with other pre-trained DL techniques, such as AlexNet, VGG16, VGG19 and ResNet50. (ii) The second DL work implements a fusion of handcrafted and learned features in the MAN to improve the classification accuracy during lung cancer assessment. This work employs serial fusion and Principal Component Analysis (PCA) based features selection to enhance the feature vector. The performance of this DL structure is tested by the benchmark lung cancer CT images of LIDC-IDRI and superior classification accuracy of >97.27% is achieved.

2019 Elsevier Ltd. All rights reserved.

1. Introduction

The lung is a vital organ in the human physiological structure, and illnesses in the lung severely can influence health conditions. This work investigates the classification of lung abnormalities, such as pneumonia and cancer using a Modified AlexNet (MAN) deep learning technique.

Pneumonia is a seasonal infectious lung diseases that can lead to life-threatening complications for children (age <5 years) and elderly individuals (age > 60 years) if not diagnosed and treated early. In clinics, pneumonia is diagnosed with a variety of imaging modalities, including chest X-Ray, CT, and MRI. While chest X-Ray radiographs are the most cost-effective diagnostic tool for pneumonia detection, the diagnosis of this disease from chest X-Rays necessitate highly skilled radiologists as these images are often overlapping with other abnormal conditions of the lungs. Manual detection of pneumonia is a time-consuming process and often leads to subjective differences, which may delay diagnosis and treatment. Moreover, the extent of the pneumonia infection may appear vague on X-Ray images. Computer-Aided-Diagnosis (CAD) practice overcomes these problems by employing Machine-Learning (ML) and Deep-Learning (DL) for automated detection of pneumonia. More recently, DL has been widely researched due to its general applicability to problems involving automated feature extraction and classification [1-3]. Convolutional Neural Network (CNN) based assessments are widely used in image classification and object detection [4]. CNNs involve spatial filters that automatically gather information of the structure embedded in the image. Unlike conventional image classification methods existing in ML, CNNs are run on images directly, a pixel-based approach, as there is no need for image pre-processing subroutines [5].

In this work, a DL framework is proposed to identify pneumonia in X-Ray radiographs using a well-known DL approach called AlexNet. Initial experimental investigation with AlexNet on chosen test images (1000 normal and 1000 pneumonia X-Rays) yielded a classification accuracy of < 87%. After implementing modifications in the final stage of the DL structure, the developed MAN technique is tested on the same dataset and a classification accuracy of 96.8% is attained with a Support-Vector-Machine (SVM) based classifier and 95.38% with Softmax. These results confirm that the proposed MAN with SVM classifier helped to attain better classification accuracy than other pre-trained DL schemes, such as AlexNet, VGG16, VGG19 and ResNet50 [6].

The World-Health-Organization (WHO) states that cancer is the second principal reason of death globally; with a predicted 9.6 million deaths in 2018. Lung cancer alone is responsible for 2.09 million cases [7]. The WHO also suggests that the mortality rate due to cancer can be reduced with early detection and effective treatment scheduling. If tumor classifications, benign or malignant are successfully recognized, then a treatment procedure, such as surgery, radiotherapy, and chemotherapy can be applied to reduce the risk of death.

Lung cancer can be diagnosed with different imaging modalities, and the Computed Tomography (CT) is one of the lowest cost and effective modalities considered in clinics to examine the condition of lungs. The manual examination of lung abnormality based on CT images is a time-consuming process requiring an experienced pulmonologist. If the lung abnormality is initially assessed by a computer-assisted technique, then the analysis report can be submitted to the pulmonologist to support the decision making and the treatment planning process [8-12].

To support this kind of diagnosis, this work aims to develop a DL technique offering better classification accuracy during the image assessment task. This study proposes MAN framework for the classification of lung CT pictures into malignant and benign

class. In this study, the DL framework is initially employed to categorize the lung CT pictures of dimension $227 \times 227 \times 3$ using learned features. The outcome of this technique yielded a result with a low value of classification accuracy (< 86 %). Hence, in this work, an Ensemble-Feature-Technique (EFT) is executed to improve the classification performance of lung CT images.

In EFT, each lung CT picture undergoes both a (i) deep feature extraction process and a (ii) handcrafted feature extraction process [6]. After extracting features from the test images, a Principal Component Analysis (PCA) based feature fusion and selection process is used to enhance the feature vector for use in training, testing, and validating the classifier. In this work, lung CT picture features are extracted with MAN. Simultaneously, the following handcrafted features are extracted as depicted in Fig 2: (i) Conversion of RGB to grayscale picture, (ii) Separating the test image into high/low contrast sections based on a threshold filter, (iii) Implementing a morphological filter to enhance the cancer section, (iv) Extracting the tumor section with morphological/watershed segmentation and (v) Extracting the Haralick and Hu moments features (27 features) of the cancerous section. After extracting the required features from the test image, a feature fusion based on the PCA is implemented to fuse the deep and handcrafted features. In this proposal, Serial fusion and PCA selection is an unique approach that adds incremental value to the Deep Learning approach for detecting lung abnormalities. Finally, these features are used to train, test and validate the classifiers, including SVM, KNN, and the RF. The result of the proposed study is confirmed and validated against other DL approaches the AlexNet, VGG16, VGG19, and ResNet50. All experiments are implemented using MATLAB, and the results of this study confirm that the MAN with the SVM classifier offers better classification accuracy (>97%) compared to other DL frameworks considered in this work.

Recently, a significant number of DL frameworks have been proposed and implemented to inspect biomedical signals and images. Of these, an extensive quantity of traditional, modified form and customary DL architecture are already proposed and implemented to examine a class of clinical-grade and benchmark medical pictures [13-17]. A detailed assessment of the existing DL methodologies and its biomedical applications can be found in [18]. From the earlier research works, it can be noted that traditional DL architectures and their modified versions are widely adopted by researchers to solve a variety of image classification problems. Earlier work also confirms that, if an adequate number of pictures are used, then it is possible to train the DL architecture in an efficient manner to attain better accuracy. Hence, in our work we have improved an existing ALEXNET approach by incorporating PCA fusion with an aim of developing a more efficient DL process.

Due to its clinical significance, a variety of DL architectures are proposed to diagnose a variety of lung abnormalities. These works considered chest X-Ray and lung CT pictures for analysis. X-Ray based assessment yields a very low accuracy due to the poor visibility of the abnormal section in radiographs compared to other modalities [19-22]. Hence, it is essential to develop an efficient DL technique providing considerable accuracy during the image classification task.

Similarly, the earlier assessment on the LIDC-IDRI dataset confirms that the existing techniques offer satisfactory results during the classification of the images into malignant and benign class [23,24]. Further, the accuracy varies based on the DL architecture and the number of images considered for the assessment. A detailed review of the assessment of the LIDC-IDRI can be found in the works of Pehrson et al. [18]. This work presents a comprehensive assessment of various ML and DL techniques implemented to classify the lung nodule pictures.

This study is prepared as follows: section 2 presents the related examination existing in the literature; proposal and implementation of the proposed DL framework is presented in section 3. Section 4 describes the investigational outcomes and discussion and finally the conclusion is presented in section 5.

2. Motivation

The research work is motivated by the Content Supported Medical Image Retrieval (CSMIR) proposed by Fernandes et al. [42]. Their approach was able to analyze the tumor or lesion from 2D and 3D radiology images. This approach was found to be very beneficial by medical practitioners in multiple countries. In their analysis of existing approaches, they summarized key advantages/shortcomings. Inspired by this summary, we have developed a deep learning-based framework to detect lung abnormalities.

3. Methodology

Lung abnormalities, such as pneumonia and cancer are primarily diagnosed based on imaging techniques, and early discovery may significantly improve patient survival rates. This work proposes two different DL frameworks to examine chest X-Rays and the lung CTs. This section presents the details of the dataset considered and the implemented DL frameworks. Finally, a section is included to discuss the Image-Performance-Metrics (IPM) considered to justify the performance of the proposed technique.

3.1 Chest X-Ray examination

Chest X-ray is a vital tool used to assess lung diseases. This work uses the radiograph images provided in Rajpurkar et al. [25] for assessment. Initially, pre-trained DL systems, such as AlexNet, Visual Geometry Group's DL networks (VGG16 and VGG19) and ResNet50 are used to classify the chosen images of the radiographs in to normal and pneumonia class with a SoftMax classifier.

Among other DL systems, the structure of AlexNet is the simplest and hence, in this work the structure of AlexNet is modified to improve the classification result. The Modified AlexNet (MAN) consist of traditional initial layers (Block1 to Block5), a flattened layer to lessen the feature vector (FVx1) and two fully connected layers to select the essential amount of the deep-learning features to train, test and the classifier. In this work, every initial block consists of convolution, ReLU, normalization, and max-pooling layers to improve the feature extraction capability. Finally, the existing SoftMax layer is replaced by a Support Vector Machine (SVM) with a linear kernel [1]. The outline of the MAN implemented in this work can be found in other recent publications [26].

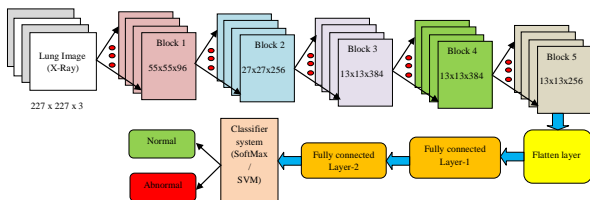


Fig. 1. Modified AlexNet architecture proposed to classify the chest X-Ray radiographs.

3.2 Lung CT examination

The DL framework implemented for CT picture examination can be found in Fig 2. This work uses the MAN network shown in Fig 1 with a handcrafted feature extraction technique. Later, the learned features are combined with the handcrafted features using a Principal Component Analysis (PCA) technique. The combined features are then used to train, test and validate the system.

3.2.1 LIDC-IDRI database

This dataset consists of clinical-grade lung CT images with various nodule sizes [8, 27, 43]. The dataset contains 1,018 slices of 1,010 cases of lung CT; This work considered 777 slices of lung nodule and remaining on-nodule.

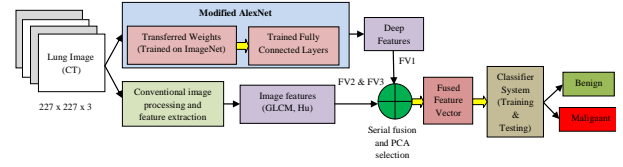


Fig. 2. Ensemble-Feature-Technique implemented to examine the LIDC-IDRI database

3.2.2 Image separation

The existing CT image is in the RGB scale, but during the assessment it is necessary to consider its grayscale version. After the conversion, these images are resized into $227 \times 227 \times 1$ pixels. Normally, in CT, along with the nodule section, other regions such as bone and heart tissues also have better visibility. Hence, in this work, a threshold filter is used to separate the vital lung sections from the test CT picture. The thresholding filter is widely adopted to separate the skull section in the brain image assessment [28-30].

The pseudo-code of the filter is as follows;

Let the trial picture consist of a gray thresholds of the range $\{0, \dots, Th-1\}$, In which the $Th=256$.

- (i) *A gray level histogram recognizes the threshold level 'TL', which segregates the bone and the heart section from the lung section.*
- (ii) *The thresholds $>TL$ can be used to extract the high contrast sections from sections)the lung CT (bone and heart)*
- (iii) *The thresholds $<TL$ extracts the low and medium contrast sections (tumor and other*

In this filter, an adaptively chosen threshold value (TL) can be used to separate the required region from the test image. In this proposed work, this filter is implemented to separate the lung section from the other unwanted sections of the CT. Later, a morphological segmentation is implemented to enhance the cancerous part of the lung, from which it can be mined using a suitable segmentation technique.

3.2.3 Nodule segmentation

Morphological segmentation and watershed segmentation are common techniques for automated nodule segmentation from the enhanced lung picture. In this work, both methods were compared, and morphological segmentation offered better performance.

3.2.4 Handcrafted feature extraction

After mining the nodule, its shape and texture features are then extracted with the Haralick and Hu approach [44]. The Haralick method helps to extract the essential information; which forms a feature-vector (FV2) with 18 vital features. The Hu moments then helps to achieve 9 related nodule features (FV3) [1,24,28]. In the ML approach, these two feature sets are sufficient to classify the test images into benign and malignant. In this DL framework, these feature sets are fused with the deep-features (FV1) in order to get a feature vector of size 1051×1 ($FV_n = FV_1 + FV_2 + FV_3$). This FV_n is achieved with the help of PCA supported features fusion technique.

3.2.5 Feature fusion and selection

In this work, the serial feature fusion is executed and the vital features are selected based by PCA. The serial features fusion technique combines the one-dimensional feature vectors, FV1 (deep-features), FV2 (Haralick) and FV3 (Hu moments) to get a new vector FVn.

Generally, the PCA transforms n-vectors (f_1, f_2, \dots, f_n) from a D-dimensional space to D' space with values $(f'_1, f'_2, \dots, f'_n)$ in which both D and D' are positive integers with a dimension $D' \leq D$.

$$\text{In PCA, the new feature will be: } f'_n = \sum_{k=1}^{D'} P_{k,i} E_k \quad (1)$$

where E_k = eigenvectors and $P_{k,i}$ = principal components. Other details on PCA can be found in [6].

The main advantage of this technique is the final feature vector (FVn) consists of the deep features and the handcrafted features, which helps to improve the classifier's performance. Earlier research confirms that the performance of the DL system can be enhanced with Ensemble-Feature-Technique (EFT) [6].

3.2.6 Classifier system and its performance evaluation

Even though a considerable number of classifiers exist, classifiers such as Support Vector Machine (SVM), K-Nearest Neighbor (KNN), and Random Forest (RF) techniques are generally used in ML techniques [1,10]. In the proposed DL technique, these classifiers are implemented instead of the typical SoftMax, to achieve better results. The performance of the proposed system is evaluated based on the essential measures of True-Positive (TP), True-Negative (TN), False-Positive (FP), and False-Negative (FN). With these parameters; other essential values, such as accuracy, precision, sensitivity, specificity, F1 score, False Positive Rate (FPR), False-Negative Rate (FNR) False Discovery Rate (FDR) and false omission rate (FOR) are also computed. The mathematical expressions of these variables can be found in [28-30].

$$\text{Accuracy} = \frac{TP + TN}{TP + TN + FP + FN} \quad (2)$$

$$\text{Precision} = \frac{TP}{TP + FP} \quad (3)$$

$$\text{Sensitivity} = \frac{TP}{TP + FN} \quad (4)$$

$$\text{Specificity} = \frac{TN}{TN + FP} \quad (5)$$

$$\text{F1Score} = \frac{2TP}{2TP + FN + FP} \quad (6)$$

$$\text{FNR} = \frac{FN}{FN + TP} \quad (7)$$

$$\text{FPR} = \frac{FP}{FP + TN} \quad (8)$$

$$\text{FDR} = \frac{FP}{FP + TP} \quad (9)$$

$$\text{FOR} = \frac{FN}{FN + TN} \quad (10)$$

4. Results and Discussions

This work considers two different image datasets: chest X-Ray (normal and pneumonia classes) and lung CT (malignant and benign classes). The proposed approach is tested on images of dimension $227 \times 227 \times 3$ pixels. The developed DL system was implemented in a workstation with a Core i5 (7th Gen) 3.1 GHz CPU (Turbo) with 8 GB RAM; 2GB graphic memory and implemented in MATLAB.

Table 1. Total number of test images considered in the proposed work

Dataset	Class	Number of Images
Chest X-Ray	Normal	1000
	Pneumonia	1000
	Total	2000
Lung cancer (LIDC-IDRI)	Malignant	1000
	Benign	500
	Total	1500

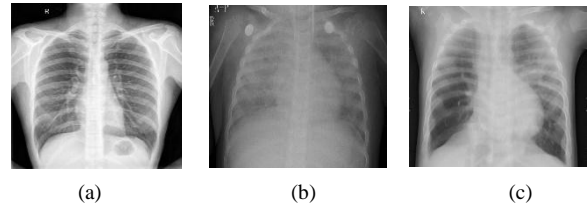


Fig. 3. Sample chest X-Ray radiographs.(a) Normal, (b) Bacterial Pneumonia, (c) Viral Pneumonia

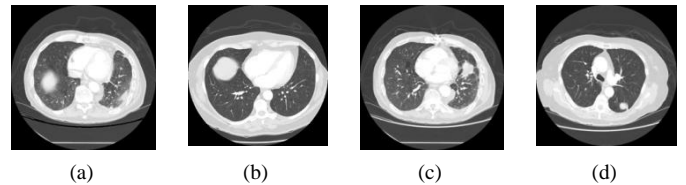
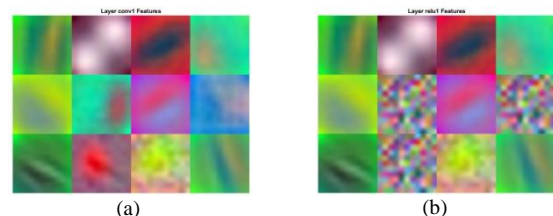


Fig. 4. Sample lung CT images of LIDC-IDRI(a) & (b) Malignant class, (c) & (d) Benign class

Fig 3 and 4 illustrates the sample test images of X-Ray radiographs and the lung CT images considered for investigation. Initially, the X-Ray database is chosen for the assessment. This database consists of images of varied dimensions; in this work, an image resizing process is implemented to reduce the dimension of the images to $227 \times 227 \times 3$ pixels. The considered dataset consists of two-dimensional (2D) pictures, which minimizes the complexity of assessment. The proposed tool is also implemented and tested on the lung CT images of the LIDC-IDRI database. LIDC-IDRI provides an RGB scale clinical grade lung CT pictures to test and validate the performance of disease examination tools, and is a standard benchmark lung dataset for the lung-nodule detection task. In this work, all the chosen images of the dataset is reduced to $227 \times 227 \times 3$ pixels to minimize the CPU run time. Further, a data augmentation is also implemented to attain 500benign class test pictures.

Primarily, a pre-trained AlexNet is used to examine the chest X-Ray images, and the performance of the AlexNet is compared against VGG16, VGG19, and ResNet50. The experimental outcome (IPMs) attained with the pre-trained AlexNet is poor compared with VGG19 and ResNet50. Hence, a modification is implemented to build a Modified AlexNet (MAN), in which the modifications are implemented in the Fully-Connected (FC) layers and the classification layer by replacing SoftMax with SVM.

Fig 5 depicts the results attained in block1. Block 1consists of multiple layers, including convolutional, Rectified Linear Unit (ReLU), normalization, and max-pooling. A similar layer structure exists the remaining blocks, Block 2 to Block5.



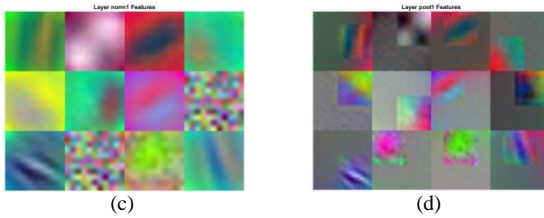


Fig.5. Various layer results of modified AlexNet block1. (a) Convolution, (b) ReLU, (c) Normalization, (d) Max-pooling

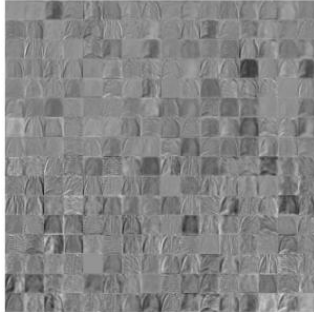


Fig.6. Activation map of the convolution layer (block5) for X-Ray images

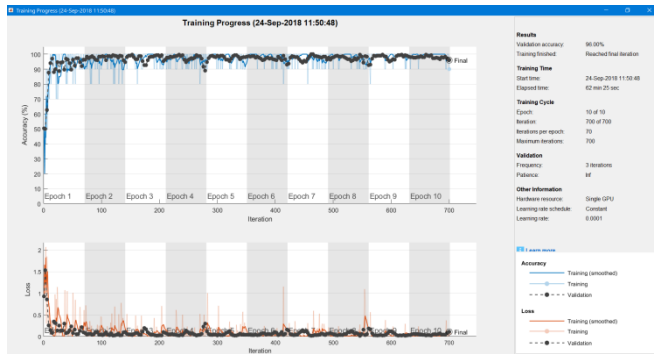


Fig. 7. The accuracy and loss function attained for the MAN-SVM.

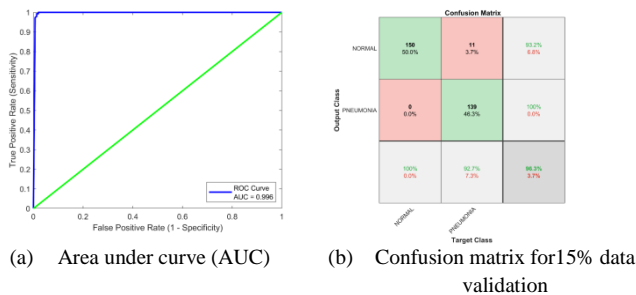


Fig.8. Experimental outcome of the testing process

Fig 6 presents the activation map of the final convolution layer available in the proposed MAN-SVM system. Among the 2000 test images (1000 normal and 1000 pneumonia), 70% (700 normal and 700 pneumonia) of the images are used to train the DL architecture and 30% (300 normal and 300 pneumonia class) of the images are used to test the MAN-SVM. Initially, 700 images (350 normal and 350 pneumonia) are used to train the MAN and also 300 images (150 normal and 150 abnormal) are used for the testing process. Fig 7 depicts the training accuracy for 10 epochs and the corresponding loss function. Fig 8 presents the Area Under Curve (AUC) and Fig 8(b) represents confusion matrix attained during the testing operation. Results presented in Fig. 8(a) through ROC curve proves that the prediction rate is highly accurate with an AUC value of 0.996. Later, 1400 images of chest X-Ray are used for training, with 600 images used for testing. The results are depicted in Table 3. This process is repeated with the other presented DL systems, based on transfer learning, and the overall results are also depicted in Table 3.

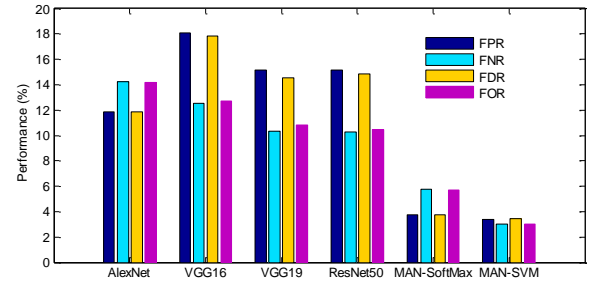


Fig. 9. Performance based validation of MAN-SVM with other DL techniques

From Fig 9, it is noted that the FPR, FNR, FDR, and the FOR attained with the MAN-SVM is better compared to the alternative techniques. This confirms that the proposed DL framework (MAN-SVM) presents better results on images in the chest X-Ray database when compared to other DL systems.

The proposed DL architecture (MAN-SVM) is then implemented to test lung cancer images of the LIDC-IDRI. In this image, the visibility/threshold value of the lung-nodule section is approximately similar to the other body organs such as the bone section and the heart. Hence, the overall performance measure attained with the LIDC-IDRI using the deep-learning feature-based classification with the SoftMax, SVM, KNN, and the RF offered satisfactory results. Recent research confirms that the Ensemble-Feature-Technique (EFT) can be implemented to enhance the performance of the DL technique. The main advantage of EFT is consideration of features extracted using conventional methods. In this work, EFT is implemented by fusing the deep-features (1024 features) with the handcrafted features of Haralick and Hu moments (27 features).

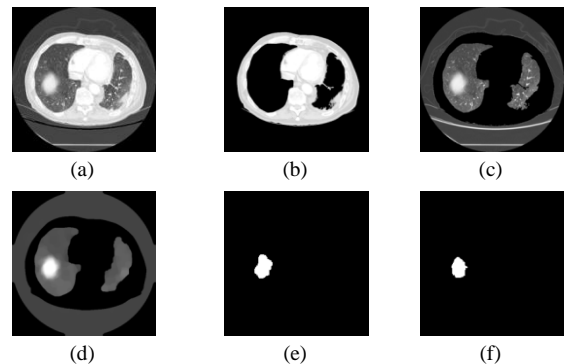


Fig.10. Initial processing of the lung CT for ensemble-feature technique. (a) Test image, (b) High resolution segment, (c) Low resolution segment, (d) Morphological filtering, (e) Morphological segmentation, (f) Watershed segmentation

Fig 10 depicts the results attained for lung CT pictures. Fig 10 (a) depicts the grayscale version of the test picture and Fig 10 (b) and (c) present the separated high and low/medium contrast sections of the test pictures, respectively. The low/medium contrast image is then enhanced with a morphological filter as in Fig 10 (d) and the nodule section is then mined with a chosen segmentation technique. Fig 10 (e) and (f) presents the nodule extracted with the morphology and the watershed technique. This section is then considered to attain the handcrafted features. In this work, the lung-nodule extracted with the morphological segmentation is considered.

In this work, the PCA based feature fusion is implemented to combine all the existing features vectors; FVI (1024×1),

FV2 (18×1) and FV3 (9×1) and the final FVn (1051×1) is considered to train, test and validate the DL framework. The overall aim of this EFT technique is to improve the classification accuracy irrespective of the classifier unit

In this work, the proposed EFT is implemented for the entire LIDC-IDRI database and the ensemble of deep and handcrafted features are then considered to obtain the best classification result with MAN-SVM, MAN-KNN and MAN-RF. The experimental outcomes are depicted in Table 2. From this table, it can be confirmed that the ensemble of features helps to achieve enhanced classification accuracy compared to other DL techniques. Hence it is evident that the objective to improve the classification accuracy, irrespective of the classifier unit, using the MAN-SVM approach was successful.

Furthermore, the performance of the MAN-SVM (E) is then validated with the other DL based results existing in the literature and these details are presented in Table 2 confirms that the proposed DL system offers better results than alternative techniques. Additionally, the performance of MAN-SVM (E) is validated with a relative assessment with the state of art techniques existing in the literature; Table 3 confirms that the proposed DL system offers better results than alternative techniques. From this table, it can also be noted that the proposed

framework helps to achieve better classification accuracy compared to other techniques existing in the literature.

Table 2. Comparison of proposed DL method with state of art methods for LIDC-IDRI database

Reference	Accuracy (%)	Sensitivity (%)	Specificity (%)
Da Silva et al. [31]	94.75	94.7	95.1
Causey et al. [32]	94.6	94.8	94.3
Ramachandran et al. [33]	93.0	89.0	-
Song et al. [34]	84.2	84.0	84.3
Han et al. [35]	82.5	96.6	71.4
Zhang et al. [36]	95.0	93.5	90.2
Xie et al. [37]	89.53	84.2	92.0
Shaffie et al. [38]	91.2	85.0	95.8
Abbas et al. [39]	95.0	94.0	96.0
Xie et al. [40]	91.6	86.5	94.0
Nibali et al. [41]	89.9	91.1	88.6
Proposed MAN-SVM (E)	97.27	98.09	95.63

Table 3. Total number of test images considered in the proposed work

Database	Features	Approach	TP	TN	FP	FN	Accuracy (%)	Precision (%)	Sensitivity (%)	Specificity (%)	F1 score (%)
Chest X-Ray	learned features	AlexNet	868	871	117	144	86.95	88.12	85.77	88.16	86.93
		VGG16	854	839	185	122	84.65	82.19	87.50	81.93	84.76
		VGG19	894	851	152	103	87.25	85.47	89.67	84.85	87.52
		ResNet50	882	863	154	101	87.25	85.14	89.73	84.86	87.37
		MAN-SoftMax	947	958	37	58	95.25	96.24	94.23	96.28	95.22
		MAN-SVM	961	975	34	30	96.80	96.58	96.97	96.63	96.78
LIDC-IDRI	learned features	AlexNet	882	367	118	133	83.27	88.20	86.90	75.67	87.54
		VGG16	894	366	106	134	84.00	89.40	86.96	77.54	88.17
		VGG19	905	373	95	127	85.20	90.50	87.69	79.70	89.07
		ResNet50	903	388	97	112	86.07	90.30	88.97	80.00	89.63
		MAN-SVM	922	375	78	125	86.47	92.20	88.06	82.78	90.08
	handcrafted + learned features	AlexNet	931	369	69	131	86.67	93.10	87.66	84.25	90.30
		MAN-SVM	978	481	22	19	97.27	97.80	98.09	95.63	97.95
		MAN-KNN	962	474	38	26	95.73	96.20	97.37	92.58	96.78
		MAN-RF	959	463	41	37	94.80	95.90	96.29	91.87	96.09

In this work, two different datasets are used to assess the proposed DL framework, and the experimental results confirm that the framework offers better results on both the datasets. Further, the lung CT images are also assessed with a DL system using an EFT technique during classification; the results achieved with this experiment confirmed that the proposed technique works well on the considered datasets.

In future, the Local Binary Pattern (LBP) [1] based features can be extracted and implemented with the EFT approach. Further, the proposed EFT approach can be extended with other DL techniques, such as the VGG16, VGG19, and ResNet50 and its performance can be compared and validated with other existing techniques in the literature.

5. Conclusion

In this work, a modified AlexNet (MAN) is proposed to evaluate lung abnormalities in considered images. This work considers

two different modality images: chest X-Rays and lung CTs. The proposed MAN is separately tested on these two image datasets. In the initial examination phase, the MAN is used to classify the chest X-Ray into normal and the pneumonia class and the proposed DL approach provides an accuracy >96%, which is greater compared to other DL techniques considered in this study. Additionally, the MAN architecture, with and without EFT, is used to classify the lung CT pictures into malignant and benign. The proposed MAN with SVM classifier achieves a classification accuracy of 86.47% and along with EFT, similar DL framework provided an accuracy of >97.27%. This study confirms the proposed MAN framework works well on the considered image datasets. Further, a relative analysis with the existing state of the art DL techniques confirms that the proposed DL system offers better accuracy compared to the existing systems.

References

- [1] Y. Wang et al., Classification of mice hepatic granuloma microscopic images based on a deep convolutional neural network. *Appl. Soft. Comput* 74 (2019) 40-50. doi: 10.1016/j.asoc.2018.10.006.
- [2] K. Lan, et al., A survey of data mining and deep learning in bioinformatics. *J. Med. Syst* 42(8) (2018) 139. doi: 10.1007/s10916-018-1003-9.
- [3] M.N.Y. Ali, et al., Adam deep learning with SOM for human sentiment classification. *International Journal of Ambient Computing and Intelligence (IJACI)*. 10(3) (2019) 92-116. doi:10.4018/IJACI.2019070106.
- [4] Q.Z. Song, L. Zhao, X.K. Luo, X.C. Dou, Using deep learning for classification of lung nodules on computed tomography images. *J. Healthc Eng* 2017 (2017) Article ID 8314740, 7 pages. doi: 10.1155/2017/8314740.
- [5] S.M. Nagi, et al. Lung nodule detection using polygon approximation and hybrid features from CT images. *Curr. Med. Imaging. Rev* 14(1) (2018) 108-117. doi: 10.2174/1573405613666170306114320.
- [6] L. Nanni, S. Ghidoni, S. Brahmam, Ensemble of convolutional neural networks for bioimage classification. *Applied Computing and Informatics*. (2018). doi: 10.1016/j.aci.2018.06.002
- [7] <https://www.who.int/news-room/fact-sheets/detail/cancer>
- [8] S.G. Armato, et al., The lung image database consortium (LIDC) and image database resource initiative (IDRI): a completed reference database of lung nodules on CT scans. *Med Phys*. 38(2) (2011) 915–931. doi: 10.1118/1.3528204.
- [9] C. Jacobs, et al., Computer-aided detection of pulmonary nodules: a comparative study using the public LIDC/IDRI database. *Eur Radiol*. 26(7) (2016) 2139-47. doi: 10.1007/s00330-015-4030-7.
- [10] L.M. Pehrson, M.B. Nielsen, C. A. Lauridsen, Automatic Pulmonary Nodule Detection Applying Deep Learning or Machine Learning Algorithms to the LIDC-IDRI Database: A Systematic Review. *Diagnostics*. 9 (2019) 29. doi: 10.3390/diagnostics9010029.
- [11] D.M. Peña, S. Luo, A.M.S. Abdelgader, Auto Diagnostics of Lung Nodules Using Minimal Characteristics Extraction Technique. *Diagnostics*. 6 (2016) 13. doi: 10.3390/diagnostics6010013.
- [12] M.F. Serj, B. Lavi, G. Hoff, D.P. Valls. A deep convolutional neural network for lung cancer diagnostic. (2018). arXiv:1804.08170v1 [cs.CV].
- [13] J-Z. Cheng, et al., Computer-aided diagnosis with deep learning architecture: applications to breast lesions in US images and pulmonary nodules in CT scans. *Sci. Rep.* 6 (2016) 24454. doi: 10.1038/srep24454.
- [14] T. Sun, R. Zhang, J. Wang, X. Li, X. Guo, Computer-aided diagnosis for early-stage lung cancer based on longitudinal and balanced data. *Plos ONE* 8 (2013) e63559.
- [15] Zech, J.R., Badgeley, M.A., Liu, M., Costa, A.B., Titano, J.J. and Oermann, E.K., 2018. Variable generalization performance of a deep learning model to detect pneumonia in chest radiographs: A cross-sectional study. *PLoS medicine* 15(11), p.e1002683.
- [16] Y. Xiao, J. Wu, Z. Lin, X. Zhou, A deep learning-based multi-model ensemble method for cancer prediction. *Comput. Meth. Prog. Bio* 153 (2018) 1-9. doi: 10.1016/j.cmpb.2017.09.005.
- [17] O. Araque et al., Enhancing deep learning sentiment analysis with ensemble techniques in social applications. *Expert Syst. Appl* 77 (2017) 236-246. Doi: 10.1016/j.eswa.2017.02.002
- [18] L.M. Pehrson, M.B. Nielsen, C.A. Lauridsen, Automatic pulmonary nodule detection applying deep learning or machine learning algorithms to the LIDC-IDRI database: A systematic review. *Diagnostics (Basel)*. 9(1) (2019) 29. doi: 10.3390/diagnostics9010029.
- [19] J. Irvin et al., CheXpert: A large chest radiograph dataset with uncertainty labels and expert comparison. (2019). arXiv:1901.07031 [cs.CV].
- [20] P. Rajpurkar, et al., CheXNet: Radiologist-level pneumonia detection on chest x-rays with deep learning. (2017). arXiv:1711.05225 [cs.CV].
- [21] Yao, Li, Poblencz, Eric, Dagunts, Dmitry, Covington, Ben, Bernard, Devon, and Lyman, Kevin. Learning to diagnose from scratch by exploiting dependencies among labels. arXiv preprint arXiv:1710.10501 (2017).
- [22] Wang, Xiaosong, Peng, Yifan, Lu, Le, Lu, Zhiyong, Bagheri, Mohammadhadi, and Summers, Ronald M. Chestx-ray: Hospital-scale chest x-ray database and benchmarks on weakly-supervised classification and localization of common thorax diseases. arXiv:1705.02315 (2017).
- [23] B.A. Skourt, A.E. Hassani, A. Majda, Lung CT image segmentation using deep neural networks. *Procedia Comput. Sci* 127 (2018) 109-113.
- [24] H. Polat, H.D. Mehr, Classification of pulmonary CT images by using hybrid 3D-deep convolutional neural network architecture. *Appl. Sci.* 9 (2019) 940. doi:10.3390/app9050940.
- [25] P. Rajpurkar, et al., Deep learning for chest radiograph diagnosis: A retrospective comparison of the CheXNeXt algorithm to practicing radiologists. *PLoS Med.* 15(11) (2018) e1002686. doi: 10.1371/journal.pmed.1002686.
- [26] T. Shanthi, R.S. Sabeenian, Modified Alexnet architecture for classification of diabetic retinopathy images. *Comput Electr. Eng* 76 (2019) 56–64.
- [27] <https://wiki.cancerimagingarchive.net/display/Public/LIDC-IDRI>
- [28] N. Dey et al., Social-group-optimization based tumor evaluation tool for clinical brain MRI of flair/DW modality. *Biocybern. Biomed. Eng* 39(3) (2019) 843-856. doi: 10.1016/j.bbe.2019.07.005.
- [29] V. Rajinikanth, N. Dey, R. Kumar, J. Panneerselvam, N.S.M. Raja, Fetal head periphery extraction from ultrasound image using Jaya algorithm and Chan-Vese segmentation. *Procedia Comput. Sci* 152 (2019) 66-73. <https://doi.org/10.1016/j.procs.2019.05.028>
- [30] V. Rajinikanth, S.C. Satapathy, S.L. Fernandes, S. Nachiappan, Entropy based segmentation of tumor from brain MR images—a study with teaching learning based optimization. *Pattern Recogn. Lett* 94 (2017) 87-95.
- [31] G.L.F Da Silva, O.P. Da Silva Neto, A.C. Silva, A.C. de Paiva, M. Gattass Lung nodules diagnosis based on evolutionary convolutional neural network. *Multimed. Tools Appl* 76 (2017) 19039–19055.
- [32] J.L. Causey, J. Zhang, S. Ma, B. Jiang, J.A. Qualls, D.G. Politte, F. Prior, S. Zhang, X. Huang, Highly accurate model for prediction of lung nodule malignancy with CT scans. *Sci. Rep.* 8 (2018) 9286. <https://doi.org/10.1038/s41598-018-27569-w>
- [33] S. Ramachandran, J. George, S. Skaria, V.V. Varun, Using YOLO based deep learning network for real time detection and localization of lung nodules from low dose CT scans. In *Proceedings of the Medical Imaging 2018: Computer-Aided Diagnosis*, Houston, TX, USA, 12–15 February 2018; Volume 53.
- [34] Q.Z Song, L. Zhao, X.X. Luo, X.C. Dou, Using Deep Learning for Classification of Lung Nodules on Computed Tomography Images. *J. Healthc. Eng* 2017 (2017) Article ID 8314740, 7 pages. <https://doi.org/10.1155/2017/8314740>
- [35] G. Han, X. Liu, G. Zheng, M. Wang, S. Huang, Automatic recognition of 3D GGO CT imaging signs through the fusion of hybrid resampling and layer-wise fine-tuning CNNs. *Med. Biol. Eng. Comput.* (2018) 2201–2212.
- [36] Zhang, T.; Zhao, J.; Luo, J.; Qiang, Y. Deep belief network for lung nodules diagnosed in CT imaging. *Int. J. Perform. Eng.* 2017, 13, 1358–1370.
- [37] Xie, Y.; Zhang, J.; Xia, Y.; Fulham, M.; Zhang, Y. Fusing texture, shape and deep model-learned information at decision level for automated classification of lung nodules on chest CT. *Inf. Fusion* 2018, 42, 102–110.
- [38] A. Shaffie, A. Soliman, L. Fraiwan, M. Ghazal, F. Taher, N. Dunlap, B. Wang, V. van Berkel, R. Keynton, A. Elmaghraby, et al., A Generalized Deep Learning-Based Diagnostic System for Early Diagnosis of Various Types of Pulmonary Nodules. *Technol. Cancer Res. Treat* (2018) 17.
- [39] Q. Abbas, Nodular-Deep: Classification of Pulmonary Nodules using Deep Neural Network. *Int. J. Med. Res. Heal. Sci* 6 (2017) 111–118.
- [40] Y. Xie, Y. Xia, J. Zhang, Y. Song, D. Feng, M. Fulham, W. Cai, Knowledge-based Collaborative Deep Learning for Benign-Malignant Lung Nodule Classification on Chest CT. *IEEE Trans. Med. Imaging* 38(4) (2019) 991-1004. doi: 10.1109/TMI.2018.2876510.
- [41] A. Nibali, Z. He, D. Wollersheim, Pulmonary nodule classification with deep residual networks. *Int. J. Comput. Assist. Radiol. Surg* 12 (2017) 1799–1808.
- [42] S.L. Fernandes, V.P. Gurupur, H. Lin, R.J. Martis, A Novel fusion approach for early lung cancer detection using computer aided diagnosis techniques. *Journal of Medical Imaging and Health Informatics* 7(8) (2017) 1841-1850.
- [43] S.M. Naqi, M. Sharif, M. Yasmin, S.L. Fernandes, Lung nodule detection using polygon approximation and hybrid features from CT images. *Current Medical Imaging Reviews* 14(1) (2018) 108-117.
- [44] Z. Huang, J. Leng, J., Analysis of Hu's Moment Invariants on Image Scaling and Rotation. *Proceedings of 2010 2nd International Conference on Computer Engineering and Technology (ICCET)*. (2010) 476-480, Chengdu, China. IEEE.